ARE NATURAL CLIMATE FORCINGS ABLE TO COUNTERACT THE PROJECTED ANTHROPOGENIC GLOBAL WARMING?

CÉDRIC BERTRAND*, JEAN-PASCAL VAN YPERSELE and ANDRÉ BERGER

Institut d'Astronomie et de Géophysique G. Lemaître, Université catholique de Louvain, 2 Chemin du Cyclotron, B-1348 Louvain-la-Neuve, Belgium
E-mail: Cedric.Bertrand@oma.be

Abstract. A two-dimensional global climate model is used to assess the climatic changes associated with the new IPCC SRES emissions scenarios and to determine which kind of changes in total solar irradiance and volcanic perturbations could mask the projected anthropogenic global warming associated to the SRES scenarios. Our results suggest that only extremely unlikely changes in total solar irradiance and/or volcanic eruptions would be able to overcome the simulated anthropogenic global warming over the century. Nevertheless, in the critical interval of the next two decades the externally-driven natural climate variability might possibly confuse the debate about temperature trends and impede detection of the anthropogenic climate change signal.

1. Introduction

There is general agreement that the average surface air temperature of the Earth has increased by about 0.6 °C over the past century, and by about 0.2° to 0.3 °C over the last 40 years (e.g., Jones, 1994; Parker et al., 1995). Studies of the statistical significance of the observed global mean surface air temperature trend over the last century have detected a significant change and have shown that the observed warming trend is unlikely to be entirely natural in origin (e.g., Lane et al., 1994; Schönwiese, 1994; Thomson, 1995; Kaufmann and Stern, 1997; Houghton et al., 2001). Further evidence comes from numerical climate simulations. They have indeed shown that accounting for human activities, that modify the atmospheric concentration of greenhouse gases (GHG) and of tropospheric sulphates, increases the models' ability to simulate the spatial and temporal pattern of the historical temperature record (e.g., Santer et al., 1996; Stott et al., 2000, 2001). Both natural and anthropogenic forcings play a role in explaining the overall global warming of the last 150 years. This must be kept in mind when trying to project future climate changes resulting from human activities. They need to be set in the context of what has happened in the past.

At decadal to century time scale, recent publications, (e.g., Bertrand and van Ypersele, 1999; Bertrand et al., 1999, 2002; Free and Robock, 1999; Crowley,

* Now at the Royal Meteorological Institute of Belgium, 3 Avenue Circulaire, B-1180 Brussels, Belgium.

Climatic Change **55:** 413–427, 2002.

2000) indicate clearly that volcanic and solar variability (changes in solar irradiance) have played an important role in the temperature variations of pre-industrial times. They have the potential to account for climates as cold as the Little Ice Age or as warm as the Medieval epoch. To what extent would they be able to mask the projected 21st century anthropogenic warming? This is what we intend to analyse using the 2-D LLN (Louvain-la-Neuve) climate model. Although future impacts of the Sun could be either negative or positive, only its potential cooling effect will be considered in the 'masking' simulations (to try counterbalancing the global warming).

2. Anthropogenic Emissions Scenarios and Climate Model Description

Until recently, the IPCC 'business as usual' scenario, IS92a (Houghton et al., 1996), was the reference for model projections of future climate change. This and the other scenarios of the Second Assessment Report (SAR) have been revised for the Third Assessment Report (TAR). The IPCC Special Report on Emissions Scenarios (SRES) (Nakićenović et al., 2000) describes indeed a new set of emission scenarios for CO_2, other greenhouse gases, and sulphate. Each scenario corresponds to a 'storyline' for population, economic growth, energy, land use, etc. Rather than providing a central value like the IS92a 'business as usual' of SAR, SRES is intended to display the uncertainty range of emission forecasts. Here, we will present climate projections up to 2100 that explore the response of the climate system to the 6 SRES Illustrative Marker Scenarios (A1B, A1T, A1FI, A2, B1, and B2). The CO_2 concentrations were calculated from the SRES Illustrative Marker Scenarios using the 'reference' version of the Bern Carbon Cycle Model (Joos et al., 2001), e.g., with an average ocean uptake for the 1980s of 2.0 PgC/yr (F. Joos, personal communication). The SRES sulphur emissions were converted to concentrations of sulphate aerosol particles using a monthly mean sulphate distribution for 2050 simulated by the Moguntia model (H. Rodhe and U. Hansson, personal communication).

Knowing the projected concentration change corresponding to these emission scenarios for the different greenhouse gases (F. Joos, personal communication), we have evaluated the associated change in effective CO_2 concentration with respect to the year 1850. Indeed, since the climate system responds slowly to external changes, the future climate response depends to some degree on the forcing history prior to now. Sensitivity tests (e.g., Fichefet and Tricot, 1992) have shown that this 'historical effect, or cold start' is a vital consideration during the first few decades, but becomes unimportant after 30–40 years of simulation. Given the low computer time requirements of our climate model, all our transient climate simulations have been started in 1850 in order to include the historical increase in equivalent CO_2.

All simulations were carried out using the Louvain-la-Neuve two-dimensional sector-averaged global climate model (Figure 1). This model (Crucifix et al., 2001,

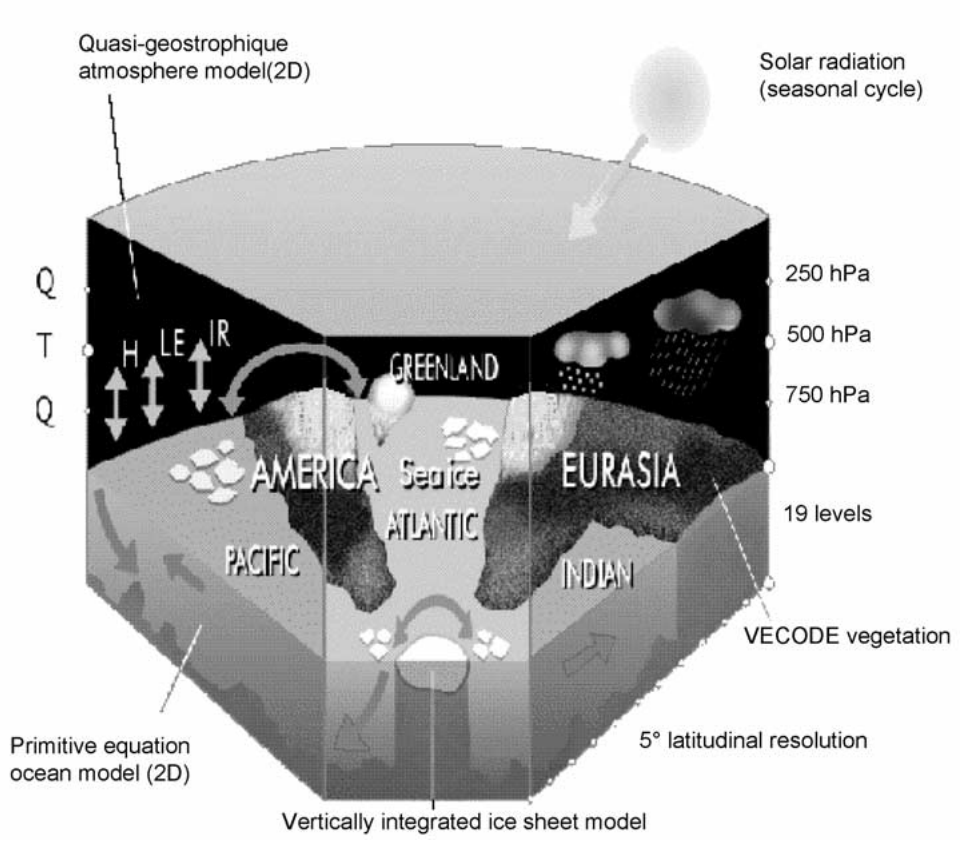

Figure 1. Sketch of the Louvain-la-Neuve two-dimensional sector-averaged global climate model. This Earth system model of intermediate complexity includes (a) a zonally averaged 2-layer atmosphere model; (b) a primitive equation, zonally averaged ocean model for the three main basins, coupled to a thermodynamic sea-ice model; (c) a land surface model applied over the two main continents (Eurasia-Africa and America), with explicit snow budget; (d) a terrestrial biosphere model with two plant functional types (trees and grass); (e) a vertically integrated ice sheet model. The atmospheric, oceanic, and land surface components have a latitudinal resolution of 5°.

2002), which links together the atmosphere, the hydrosphere, the terrestrial surface and the cryosphere of both hemispheres is latitude, altitude, and time-dependent. The atmosphere is zonally averaged (i.e., it is a latitute-altitude model) and discretized on a 5° latitudinal grid. The atmosphere dynamics (Gallée et al., 1991) is represented by a zonally averaged two-level quasi-geostrophic model. The model explicitly incorporates detailed long- and short-wave radiative transfer. Unlike the atmospheric dynamics, the radiative transfer computation uses 10 to 15 layers. The surface of each latitude belt is divided into a maximum of 13 sector types. The Eurasian continent and the American continent are represented. The VECODE model (Brovkin et al., 1997) provides for each continent and each latitude the relative cover of tree, grass and potential desert. The ocean model (Hovine and

Fichefet, 1994) has a 5° latitudinal grid with a 19 level vertical resolution and its dynamics is based on primitive equations, zonally averaged in each oceanic basin (Atlantic, Pacific, and Indian). A simple thermodynamic-dynamic sea-ice model is coupled to the ocean model. The model time step is 2 days and its sensitivity to a doubled atmospheric CO_2 concentration is 2.8 °C, which is in the middle range of the IPCC estimate.

As illustrated in Figure 1, our climate model is of intermediate complexity between one- or two-dimensional Energy Balance Models (EBM) and General Circulation Model (GCM). It allows a response varying with latitude and takes into account the main climatic processes while still being simple enough to require reasonable computer time. As an example, this model needs less than one hour of CPU time to simulate 100 ears while using a GCM still requires about one month of CPU time (using a multi-processor Fujitsu computer). The principal drawback of the quasi-geostrophic equations is their weakness in representing the tropical atmospheric dynamics, but their major advantage over primitive equations is that their zonal averaging allows a 2-day time step, comparable to that used in the EBMs. Moreover, the explicit treatment of the thermal wind equation allows the simulation of the zonal wind speed and consequently a more realistic coupling between the atmosphere and the oceanic mixed layer than in EBMs. An advantage of using such type of model is that it is much simpler than a full GCM, and therefore easier to understand and analyse. It allows the major features of the GCM response to be captured using a few basic parameters, which can be varied to carry out sensitivity experiments. As an example, sensitivity tests and many experiments to reproduce past climates (e.g., Berger and Loutre, 1997) have clearly shown the major role played in particular by the water vapor and albedo-temperature feedbacks, by the interaction between vegetation and albedo of the snow covered land surfaces, and by processus related to sea level, ice sheets and the lithosphere. Its main limitations are that it is too simple to represent the full range of interactions and nonlinear feedbacks occurring in a GCM.

While our climate model is designed to simulate the seasonal cycle of both hemispheres and allows a response varying in latitude, we have focused our attention in this paper on annual and global mean quantities. Starting from the reconstructed 1850 initial conditions, the model was first run until the ocean circulation and the seasonal cycle reached equilibrium (10000 years run). Then, using this solution as a new initial state, the model was then integrated from 1850 to 2100. From 1850 to 1990 the model was forced by the combination of (1) historical total solar irradiance (TSI) variations using the Lean et al. (1995) reconstructed TSI time series; (2) large volcanic perturbations as provided by the stratospheric aerosol optical depth data set of Sato et al. (1993); (3) anthropogenic changes of sulphate aerosol concentration; (4) anthropogenic increase of greenhouse gas (GHG) concentration. The spatial and temporal distributions of sulphate aerosol concentration used in our transient climate simulation were generated from monthly mean sulphate abundance simulated by the Moguntia model (Langner and Rodhe, 1991)

corresponding to the pre-industrial (1850) and to the industrial (1980) cases. Then, the time dependence and geographical distribution of sulphate concentration for the period between 1850 and 1990 was obtained by the use of the historical worldwide anthropogenic sulphur emission inventory of Örn et al. (1996).

3. Response to the SRES

Figure 2 displays the transient response of the annual global mean surface air temperature to the 6 SRES Illustrative Marker Scenarios with (GHG + SO_4) and without (SO_4 = 1990) changes in anthropogenic sulphate aerosol concentration beyond 1990, while prior to this date (left side of Figure 2), the thick black line exhibits the ability of our climate model to simulate the annual and global mean surface air temperature as recorded (thin black line) over the past 150 years when forced by the combination of both natural (solar and volcanic activities) and anthropogenic (atmospheric greenhouse gas concentration and tropospheric sulphate burden) factors. As we see, in spite of its limitations the model is able to capture the global temperature trend over this time period. The major discrepancy between the simulated and recorded temperature curves occurs in the vicinity of the Krakatau eruption in 1883. This could result from an overestimation of the Krakatau perturbation in the Sato et al. (1993) time series used here to account for the volcanic forcing. Indeed, such a disagreement is largely reduced when forcing the model with the Crowley (2000) volcanic time series as discussed in Bertrand et al. (2002).

In addition to the SRES Illustrative Marker Scenarios, the model response to the IPCC IS92a emission scenario is also reported in the second part of our Figure 2 for comparison. The SAR labeled curve in this figure (the upper thin black line on Figure 2 right side) refers to the model response to the IS92a scenario of the IPCC Second Assessement Report, whereas the TAR curve (the lower thin black line on Figure 2 right side) is the model response to the IS92a emissions but using the new generation of chemistry and carbon cycle models (e.g., new feedbacks on the lifetimes) to determine the atmospheric GHG concentration. The largest warming of 3.1 °C simulated here is for the fossil fuel intensive (A1FI) scenario of the A1 SRES family. The lowest temperature change of about 1.6 °C is simulated for the B1 scenario family which accounts for rapid changes in economic structures toward a service and information economy, with reductions in material intensity, and the introduction of clean and resource-efficient technologies. Clearly, if anthropogenic sulphate forcing has been able to mask part of the GHG forcing over the last decades, its influence expected from the SRES and IS92a simulations on the global mean temperature from 2000 to the end of the 21st century is insignificant compared to the warming induced by the GHG. This is specially true when forcing the model with the SRES rather than with the IS92 scenarios. Indeed, emissions of sulphur dioxide, which produce sulphate aerosols, are substantially lower in SRES than in IS92. As sulphur emission controls in power plants are projected to

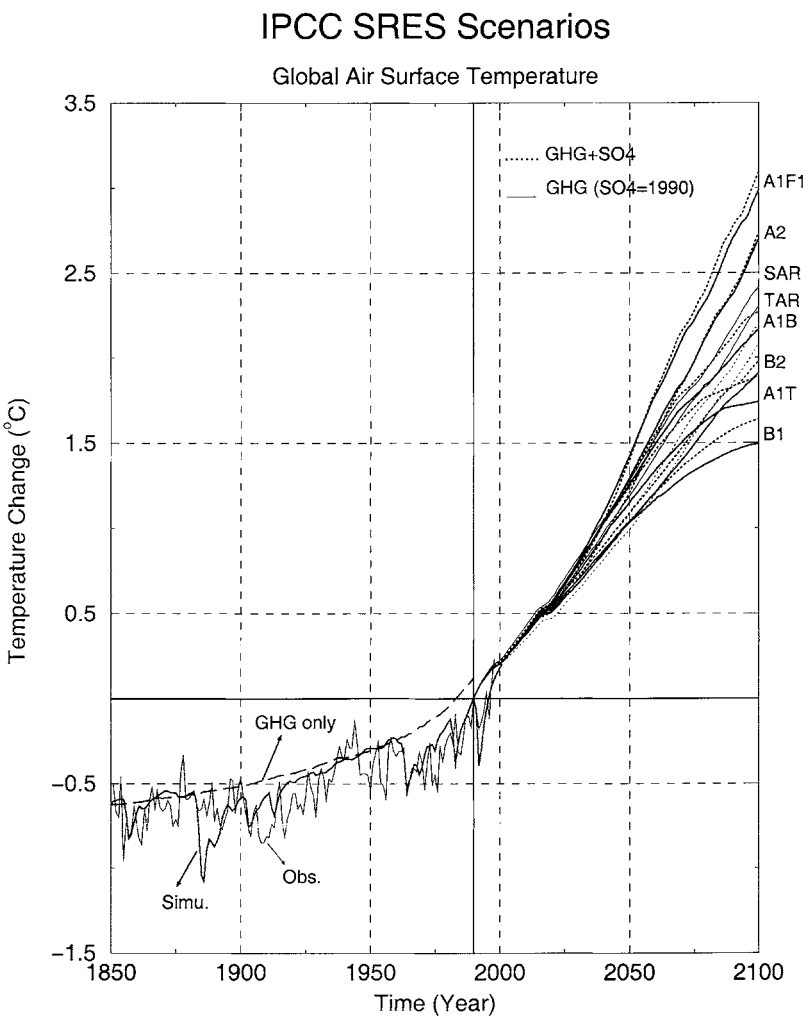

Figure 2. Annual global mean surface temperature changes from 1990 to 2100 simulated with the 2-D LLN climate model for the six SRES Illustrative Marker Scenarios (A1B, A1T, A1FI, A2, B1, and B2) and IS92a scenario with changing (dotted lines) (GHG + SO_4) and constant (solid lines) (SO_4 = 1990) aerosol concentration beyond 1990. Also displayed (on the left figure side) is the comparison (1850–1999) between the simulated annual global mean temperature response (thick black line) to the combined anthropogenic (anthropogenic sulphate aerosol and greenhouse gas) and natural (solar and volcanic) climate forcings with the recorded temperature fluctuations (thin black line) (Jones, 1994 updated; Parker et al., 1995 updated). The model response to the GHG forcing only over the past 150 years is also provided for illustration (thick long dashed line).

reduce the aerosol cooling, the global warming resulting from greenhouse gases is 'unmasked' in SRES simulations to a greater extent than in IS92a during the 21st century. This is highlighted in Figure 2 by the additional warming seen in SRES simulations when changes in sulphate concentration after 1990 (thick dotted lines) are taken into account, compared to simulations where the sulphate is kept fixed to its 1990 value (solid lines). It is the reverse for the IS92a emission scenario for which including changes in sulphur emissions after 1990 (thin dotted lines) reduces the global warming by about 0.2 °C.

4. Natural Forcings to Counteract SRES

The purpose is now to evaluate which natural factors might counteract these projected temperature changes due to human activity. Since future variations in natural forcings due to volcanic aerosols and solar variability cannot be predicted, only hypothetical scenarios can be investigated. For example, total solar irradiance will be reduced by respectively 0.41 and 1.4% in 2100 relative to its 1990 value. As illustrated in Figure 3a, these two TSI reductions correspond to the smallest and largest amplitude of the TSI variation over the last millennium as reconstructed by Bard et al. (2000) from historical record of ^{14}C and ^{10}Be. The 0.41% variation correspond to a TSI reconstruction based on factors derived from Lean et al. (1995) while the 1.4% variation is obtained when scaling the cosmogenic nuclide production rates to the Reid (1997) TSI reconstruction. The scenarios for TSI decrease over the 21st century are obtained by a simple linear interpolation between the 1990 and 2100 TSI values as illustrated in Figure 3b. By comparison, it must be noted that during the last 11-year solar cycle, the maximum magnitude of the irradiance variation recorded by satellites only accounted for a 0.1% TSI change. However, it is not at all certain that satellite measurements have captured the full range of the Sun's variability. The variation of the peaks in successive 11-year sunspot cycles shows, for example, evidence of a periodicity of around 88 years often termed the Gleissberg cycle. Over still longer time scales, there is evidence for protracted periods of enhanced activity and of extensive quiescence, for example, during the Maunder Minimum (Eddy, 1976, 1988). Moreover, estimates from solar models of the potential changes in solar variability hypothesize amplitudes in the order of 0.24–0.30% at the centennial time scales (e.g., Hoyt and Schatten, 1993; Lean et al., 1995). Therefore, the solar irradiance reduction scenarios we consider are largely in and above the upper range of solar variability at the secular time scale.

Model responses to these solar forcing scenarios combined with the larger (A1FI) and smaller (B1) responses to the SRES emission scenarios are provided in Figure 3 (panel C exhibits the model response when using SRES A1FI and panel D when using SRES B1). As we see, none of our extremely generous scenarios of solar irradiance reduction allows a stabilization of the Earth surface air temperature to its 1990 annual global mean value before 2100 when combined

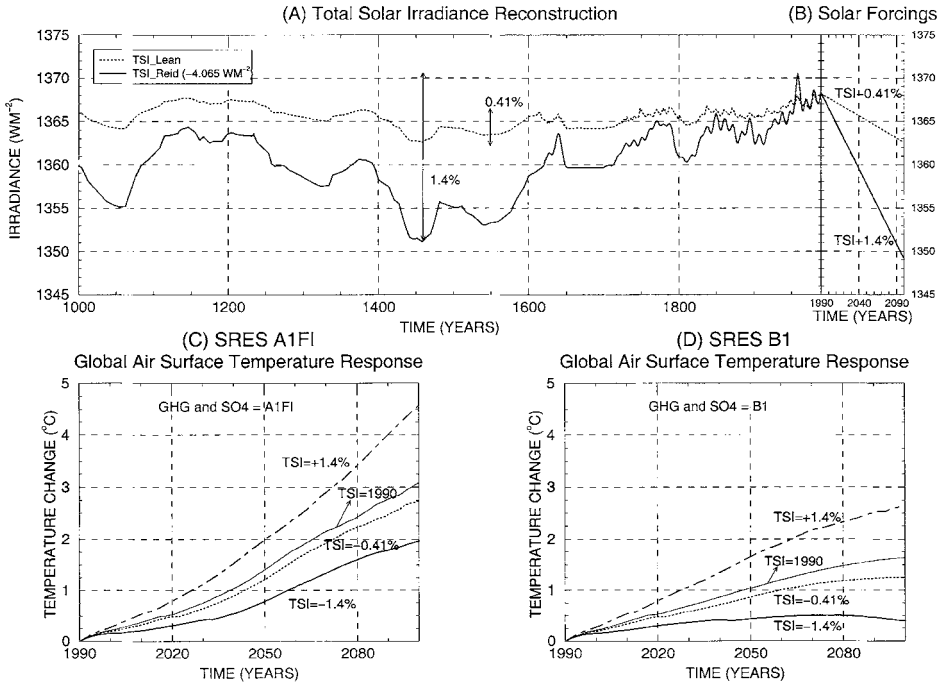

Figure 3. Solar forcing and SRES emission scenarios. (A) Upper (TSI_Reid) and lower (TSI_Lean) total solar irradiance reconstruction over the last millennium as reconstructed by Bard et al. (2000) from historical record of ^{14}C and ^{10}Be. (B) 21st century linear total solar irradiance reductions of respectively 1.4% and 0.41% as deduced from the differences between the largest and smallest TSI values in both reconstructions (A). Global annual mean surface air temperature response to these TSI reductions combined to the SRES A1FI emission scenario is displayed in panel (C) while the same is provided in panel (D) for SRES B1. The thin black curve on both bottom panels provides the model response to the corresponding SRES emission scenarios using a TSI fixed to its 1990 value (TSI = 1990). Also provided for illustration (dot-dashed curves on bottom panels) is the model response when combining the 2 SRES emission scenarios with a TSI increase of 1.4% (TSI = +1.4%).

with anthropogenic forcings. The fairly extreme TSI decrease of 1.4% allows for a simulated net global warming in 2100 of 0.4 °C over the 1990 temperature i.e., a reduction by a factor of four compared to the net global warming simulated in response to SRES B1 (1.64 °C) (Figure 3d) with TSI kept fixed to its 1990 value. When combined with A1FI the global warming is reduced from 3.09 to 1.97 °C i.e., a factor of 1.57 (Figure 3c). Using the 0.41% TSI reduction scenario accounts only for a global warming reduction in 2100 of respectively 0.35 °C when combined with A1FI (Figure 3c) and 0.38 °C with B1 SRES (Figure 3d). The dot-dashed curves in Figures 3c,d illustrate the climate model response if TSI increases by 1.4% from 1990 to 2100.

Volcanic eruptions being distributed unevenly in time, future volcanic perturbations are even more unpredictable than solar activity. Nevertheless, using the statistical properties of a 600-year long ice core record of climatically signifi-

cant volcanic eruptions in the Northern Hemisphere, Hyde and Crowley (2000) concluded that the probability of one or two eruptions with a radiative impact of -1 Wm^{-2} or larger to occur in the next 10 years is about 37% and 15% respectively (the probability of no such eruptions in a given decade being around 44%). They also estimated that the odds of a Pinatubo-scale eruption (-3 Wm^{-2} or greater) in the next decade are 15%–25%. Therefore, based on this last probability level, we have first forced the model with a scenario assuming a volcanic perturbation similar to the Pinatubo one every six years (solid curve in the top panels of Figure 4). The 6-year time interval is chosen in order to allow for a wash out of the stratospheric volcanic aerosols from one eruption to the other. Figure 4 reveals that such a periodic forcing only has a limited impact on the simulated surface air temperature. Compared to the response to A1FI and B1 respectively (Figure 2), the impact of such a volcanic activity is very small and the simulated global warming is only reduced by about 0.75 °C in 2100 for A1FI and a bit less for B1 (see the thick black curve on bottom panels in Figure 4).

In a second step, the climate model was run in a trial and error mode to determine the stratospheric volcanic aerosols burden able to counteract the temperature response to A1FI and B1. The dot-dashed curves in the top panels of Figure 4 represent such a best guess time evolution of the stratospheric aerosol burden (expressed in terms of stratospheric aerosol optical depth perturbation) needed to keep continuously the temperature at its 1990 level. Approximately twenty simulations per scenario were needed to produce these curves. Clearly, keeping temperature at its 1990 level requires a huge amount of volcanic injections in the stratosphere in comparison to the 1991 Pinatubo eruption. Moreover, only the volcanic scenario computed to counteract SRES B1 reaches a stabilization of aerosol optical depth (over the last decades of the 21st century). In contrast, the volcanic scenario computed to counteract SRES A1FI requires a volcanic activity increasing with time (see top panel in Figure 4a).

This is confirmed by performing additional model runs in which the stratospheric aerosol optical depths integrated over the time period 1990–2100 are kept identical to the best guess scenario, but distributed homogeneously throughout the simulation period. The long-dashed curves on top panels in Figure 4 display this third volcanic forcing scenario. After a cooling period the model simulates a net global warming which reaches about 1.2 °C (SRES A1FI case, panel A bottom) and 0.4 °C (SRES B1 case, panel B bottom) in 2100 relative to 1990.

Finally, sensitivity experiments have been performed in which the magnitude of the volcanic perturbation as a function of time has been kept equal to the best guess (dot-dashed curves of second scenario), but allowing now for a stratospheric cleaning from one volcanic eruption to the next with a base period of 6 years (dotted curves in Figure 4). While the model response leads to a reduction in 2100 of the net global warming by about 1 °C (SRES A1F1) and 0.2 °C (SRES B1) in comparison to the periodic Pinatubo forcing (first scenario, solid curves in Figure 4), such a volcanic scenario is clearly unable to mask the anthropogenic global warming.

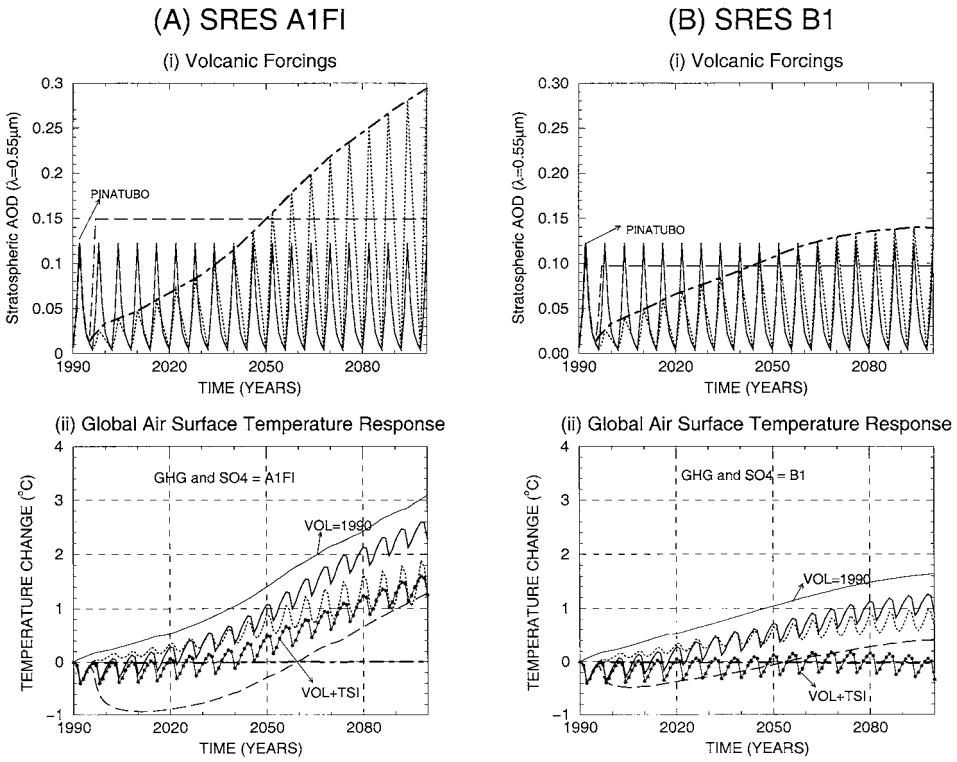

Figure 4. Volcanic forcing and SRES emission scenarios. The top panels give the volcanic forcings time series used and the bottom panels the annual and global mean surface air temperature response to these volcanic scenarios when combined with (A) the SRES A1FI and (B) the B1 Illustrative Marker Scenarios as simulated with the 2-D LLN model. The dot-dashed curves in the top panels provide the best guess time series of stratospheric aerosol optical depth needed to counteract the temperature response to (A) A1FI and (B) B1 respectively. The long-dashed curves display the volcanic perturbations which integrated over the time period 1990–2100 are kept identical to the best guess scenario but distributed homogeneously throughout the simulation period. By contrast, the dotted curves present the volcanic perturbations time series in which the magnitude of the volcanic perturbation in function of time has been kept equal to the best guess. The solid curve in top panels is a scenario assuming a volcanic perturbation similar to the Pinatubo one every six years. The thin black line on bottom panels (VOL = 1990) provides the model response to the corresponding SRES emission scenarios using a volcanic aerosol optical depth fixed to its 1990 value. Finally, the thin black curves with stars (VOL + TSI) on bottom panels display the model response when forced by the combination of a Pinatubo like eruption every six years and, a TSI decrease of 1.4% and, the corresponding SRES emission scenario.

Dotted curves on the bottom panels in Figure 4 indicate a warming of 0.7 to 1.2 °C by the end of the 21st century. This highlights the need to maintain a permanent level of high stratospheric aerosol optical depth (and therefore a permanent level of high volcanic activity) if the anthropogenic global warming has to be overcome.

When solar and volcanic activities are combined together, a Pinatubo like eruption every 6 years and a TSI decrease of 1.4% are however able to mask the global warming over the next 2 decades or at least significantly influence the evolution of the anthropogenic signal on the Earth surface temperature (thin black curves with stars on bottom panels in Figure 4). In regard to the Hyde and Crowley's work a Pinatubo like eruption has a reasonable chance to occur during such a time interval and while a TSI reduction rate of 1.4% by century over a whole century is fairly extreme, such a rate of reduction over a decade or two appears much more likely. Since detection and attribution of the anthropogenic signal have to be done against the background of the natural variability of the Earth system, such a result indicates that externally-driven natural climate variability could confuse the debate about temperature trends and render detection of the anthropogenic climate change signal more difficult.

5. Final Remarks and Conclusion

Forcing a two-dimensional sector-averaged global climate model with the 6 SRES Illustrative Marker Scenarios leads to a simulated net global warming (2100–1990) ranging from 1.6 to 3.1 °C well within the range of all the model results compiled in IPCC (Houghton et al., 2001). By contrast to the previous IPCC IS92 emission scenarios, accounting for SO_2 emissions increases the warming rate as compared to a constant 1990 level since sulphur emissions are substantially lower in the new set of emission scenarios than in the previous ones. Sensitivity experiments indicate that a level of solar variability as reconstructed over the past 1000 years is insufficient to mask the predicted 21st century anthropogenic global warming. Volcanic forcing could counteract the anthropogenic greenhouse warming, but this requires (i) a permanent level of very high volcanic activity, (ii) a volcanic forcing increasing with time, (iii) a huge stratospheric aerosol burden (unlike anything we have seen in the recent past).

Therefore, our results suggest that the dominant cause of climate change over the 21st century is likely to be changes in atmospheric trace-gas concentrations. Indeed, the number and magnitude of volcanic eruptions and the drastic reduction in the solar energy output required to mask the anthropogenic signal in our sensitivity experiments indicate that they are extremely unlikely over the 21st century. These external factors will primarily generate a natural variability of the order of 0.2 to 0.5 °C superimposed on the greenhouse warming trend. However, our results indicate that over the next two decades there is some chance that externally driven natural climate variability would mask or at least influence the evolution of the anthropogenic GHG signal. This is susceptible to delay the time when the global warming will definitely overcome the natural variability, which will inevitably confuse the debate about temperature trends and impede an early detection of the human induced warming.

Finally, limitations of the 2-D LLN model must be kept in mind. It cannot account for the possibility that volcanoes might induce or enhance El Niños (Handler, 1986; Rind et al., 1992), affect the stratosphere-troposphere interactions so as to increase the flow of marine air over the continents in winter (Robock and Mao, 1992; Kodera, 1993; Graf et al., 1993, 1994; Kodera and Yamazaki, 1994) or induce an additional climate forcing by seeding cirrus clouds (Jensen and Toon, 1992; Sassen et al., 1995; Wang et al., 1995). In addition, it is worth pointing out that various mechanisms not taken into account in the present version of our model have been proposed that might amplify the climatic impact of solar activity when seen from TSI alone. Haigh (1994, 1996) discussed the role of stratospheric ozone in modulating the solar radiative forcing of climate by a possible UV-ozone-dynamics feedback; Svensmark and Friis-Christensen (1997) proposed a cosmic-ray-clouds feedback after noting a similarity between cloudiness over the mid- to low-latitude oceans and cosmic ray flux intensity. Once again, a simple atmospheric dynamics, the absence of a cloud microphysics sheme and a solar radiative transfer averaged over the entire solar spectrum do not allow us to account for an UV-ozone-dynamics (or hypothetical⋆ cosmic-ray-clouds) feedback in our transient climate simulations. Therefore, we suggest that, taking advantage of the stratospheric aerosol optical depth trajectories determined in this study to save CPU time, more sophisticated 3-D atmosphere-ocean models must be used to test the reliability of our results. It is indeed important for decision and policymakers to confirm whether or not the occurrence of only extremely unlikely natural events might mask the predicted anthropogenic global warming of the 21st century.

Acknowledgements

We thank H. Rodhe and U. Hansson for having provided us with the data from the MOGUNTIA model and for the anthropogenic sulphur emission data set, J. Lean for her total solar irradiance reconstruction, M. Sato for her stratospheric aerosol optical depth time series and M. Crucifix for providing us with his 3-D sketch of the Louvain-la-Neuve 2-D sector-averaged global climate model. Comments by M. Allen and two anonymous referees are gratefully acknowledged. This research was partly funded by the Impulse Programme 'Global Change and Sustainable Development' (Contract CG/DD/242, Belgian State, Prime Minister's Office, Federal Office for Scientific, Technical and Cultural Affairs). Cédric Bertrand is scientific research worker with the Belgium National Fund for Scientific Research.

⋆ We speak about a *hypothetical* cosmic-ray-clouds feedback since further spatial and temporal analyses performed by Farrar (2000) over the same ISCCP C2 data as used by Svensmark and Friis-Christensen (1997) reveal that the cloud cover variation patterns are those to be expected for the atmospheric circulation changes characteristic of El Niño, weakening the case for cosmic rays as a climatic forcing factor. Moreover, the IPCC noted in its Third Assessment Report that 'mechanisms for the amplification of solar forcing are not well established' and that 'there is insufficient evidence to confirm that cloud cover responds to solar variability' (Houghton et al., 2001).

References

Bard, E., Raisbeck, G., Yiou, F., and Jouzel, J.: 2000, 'Solar Irradiance during the Last 1200 Years Based on Cosmogenic Nuclides', *Tellus* **52(B)**, 985–992.

Berger, A. and Loutre, M.-F.: 1997, 'Paleoclimate Sensitivity to CO_2 and Insolation', *Ambio* **26**, 32–37.

Bertrand, C., Loutre, M.-F., Crucifix, M., and Berger, A.: 2002, 'Climate of the Last Millennium: A Sensitivity Study', *Tellus* **54A**, 221–244.

Bertrand, C. and van Ypersele, J.-P.: 1999, 'Potential Role of Solar Variability as an Agent for Climate Change', *Clim. Change* **43**, 387–411.

Bertrand, C., van Ypersele, J.-P., and Berger, A.: 1999, 'Volcanic and Solar Impacts on Climate Since 1700', *Clim. Dyn.* **15**, 355–367.

Brovkin, V., Ganopolski, V., and Svirezhev, Y.: 1997, 'A Continuous Climate-vegetation Classification for Use in Climate-biosphere Studies', *Ecol. Modelling* **101**, 251–261.

Crowley, T. J.: 2000, 'Causes of Climate Change over the Past 1000 Years', *Science* **289**, 270–277.

Crowley, T. J. and Kim, K.-Y.: 1999, 'Modeling the Temperature Response to Forced Climate over the Last Six Centuries', *Geophys. Res. Lett.* **26**, 1901–1904.

Crucifix, M., Loutre, M.-F., Tulkens, Ph., Fichefet, Th., and Berger, A.: 2002, 'Climate Evolution during the Holocene: An Approach with an Earth System Model of Intermediate Complexity', *Clim. Dyn.* **19**, 43–60.

Crucifix, M., Tulkens, Ph., and Berger, A.: 2001, 'Modelling Abrupt Climatic Change during the Last Glaciation', in Seidov, B., Maslin, M., and Haupt, B. J. (eds.), *The Oceans and Rapid Climatic Changes: Past, Present and Future*, *AGU Geophysical Monograph* **126**, 117–134.

Eddy, J. A.: 1976, 'The Maunder Minimum', *Science* **192**, 1189–1202.

Eddy, J. A.: 1988, 'Variability of the Present and Ancient Sun: A Test of Solar Uniformitarianism', in Stephenson, F. R. and Wolfendale, A. (eds.), *Secular Solar and Geomagnetic Variations*, Dordrecht, pp. 1–23.

Farrar, P. D.: 2000, 'Do Cosmic Rays Influence Oceanic Cloud Coverage – Or Is It Only El Niño?', *Clim. Change* **47**, 7–15.

Fichefet, Th. and Tricot, Ch.: 1992, 'Influence of the Starting Date of Model Integration on Projections of Greenhouse Gas Induced Climate Change', *Geophys. Res. Lett.* **19**, 1771–1774.

Free, M. and Robock, A.: 1999, 'Global Warming in the Context of the Little Ice Age', *J. Geophys. Res.* **104**, 19,057–19,070.

Gallée, H., van Ypersele, J.-P., Fichefet, Th., Tricot, Ch., and Berger, A.: 1991, 'Simulation of the Last Glacial Cycle by a Coupled, Sectorially Averaged Climate-Ice Sheet Model I. The Climate Model', *J. Geophys. Res.* **96**, 13,139–13,163.

Graf, H. F., Kirchner, I., Robock, A., and Schult, I.: 1993, 'Pinatubo Eruption Winter Climate Effects: Model Versus Observations', *Clim. Dyn.* **9**, 81–93.

Graf, H. F., Perlwitz, J., and Kirchner, I.: 1994, 'Northern Hemisphere Tropospheric Mid-latitude Circulation after Violent Volcanic Eruptions', *Contrib. Atmos. Phys.* **67**, 3–13.

Haigh, J. D.: 1994, 'The Role of Stratospheric Ozone in Modulating the Solar Radiative Forcing of Climate', *Nature* **370**, 544–546.

Haigh, J. D.: 1996, 'The Impact of Solar Variability on Climate', *Science* **272**, 982–989.

Handler, P.: 1986, 'Possible Association between the Climatic Effects of Stratospheric Aerosols and Sea Surface Temperatures in the Eastern Tropical Pacific Ocean', *J. Climatol.* **6**, 31–41.

Houghton, J. T, Ding, Y., Griggs, D. J., Noguer, M., van der Linden, P., Dai, X., Maskell, K., and Johnson, C. I. (eds.), *Climate Change 2001: The Scientific Basis*, Contribution of Working Group I to the Third Assessment Report of the Intergovernmental Panel on Climate Change, Cambridge University Press, Cambridge, p. 944.

Houghton, J. T., Meira Filho, L. G., Callander, B. A., Harris, N., Kattenberg, A., and Maskell, K. (eds.): 1996, *Climate Change 1995: The Science of Climate Change*, Cambridge University Press, Cambridge, p. 572.

Hovine, S. and Fichefet, Th.: 1994, 'A Zonally Averaged, Three-basin Ocean Circulation Model for Climate Studies, *Clim. Dyn.* **10**, 313–331.

Hoyt, D. V. and Schatten, K. H.: 1993, 'A Discussion of Plausible Solar Irradiance Variations, 1700–1992', *J. Geophys. Res.* **98**, 18,895–18,906.

Hyde, W. T. and Crowley, T. J.: 2000, 'Probability of Future Climatically Significant Volcanic Eruptions', *J. Climate* **13**, 1445–1450.

Jensen, E. G. and Toon, O. B.: 1992, 'The Potential Effects of Volcanic Aerosols on Cirrus Cloud Microphysics', *Geophys. Res. Lett.* **19**, 1759–1762.

Jones, P. D.: 1994, 'Hemispheric Surface Air Temperature Variations: A Reanalysis and an Update to 1993', *J. Climate* **7**, 1794–1802.

Joos, F., Prentice, C. I., Sitch, S., Meyer, R., Hooss, G., Plattner, G.-K., Gerber, S., and Hasselmann, K.: 2001, 'Global Warming Feedbacks on Terrestrial Carbon Uptake Under the IPCC Emission Scenarios', *Global Biogeochem. Cycles* **15**, 891–908.

Kaufmann, R. K. and Stern, D. I.: 1997, 'Evidence for Human Influence on Climate from Hemispheric Temperature Relations', *Nature* **388**, 39–44.

Kodera, K.: 1993, 'Influence of the Stratospheric Circulation Change on the Troposphere in the Northern Hemisphere Winter', in Chanin, M. L. (ed.), *The Role of the Stratosphere in Global Change*, Springer-Verlag, Berlin, pp. 227-243.

Kodera, K. and Yamazaki, K.: 1994, 'A Possible Influence of Recent Polar Stratospheric Coolings on the Troposphere in the Northern Hemisphere Winter, *Geophys. Res. Lett.* **21**, 809–812.

Lane, L. J., Nichols, M. H., and Osborn, H. B.: 1994, 'Time Series Analysis of Global Change Data', *Environ. Pollut.* **83**, 63–88.

Langner, J. and Rodhe, H.: 1991, 'A Global Three-Dimensional Model of the Tropospheric Sulphur Cycle', *J. Atmos. Chem.* **13**, 225–263.

Lean, J., Beer, J., and Bradley, R.: 1995, 'Reconstruction of Solar Irradiance Since 1600: Implications for Climate Change', *Geophys. Res. Lett.* **22**, 3195–3198.

Nakićenović, N., Davidson, O., Davis, G., Grübler, A., Kram, T., Lebre La Rovere, E., Metz, B., Morita, T., Pepper, W., Pitcher, H., Sankovski, A., Shukla, P., Swart, R., Watson, R., and Dadi, Z.: 2000, *IPCC Special Report on Emissions Scenarios*, Cambridge University Press, Cambridge, New York.

Örn, G., Hansson, U., and Rodhe, H.: 1996, *Historical Worldwide Emissions of Anthropogenic Sulfur: 1860–1985*, Report CM-91, ISSN 0280-445X, Department of Meteorology, Stockholm University, International Meteorological Institute in Stockholm, Sweden, p. 20.

Parker, D. E., Folland, C. K., and Jackson, M.: 1995, 'Marine Surface Temperature: Observed Variations and Data Requirements, *Clim. Change* **31**, 559–600.

Reid, G. C.: 1997, 'Solar Forcing of Global Climate Change Since the Mid-17th Century', *Clim. Change* **37**, 391–405.

Rind, D., Balachandran, N. K., and Suozzo, R.: 1992, 'Climate Change and the Middle Atmosphere Part II: The Impact of Volcanic Aerosols', *J. Climate* **5**, 189–208.

Robock, A. and Mao, J.: 1992, 'Winter Warming from Large Volcanic Eruptions', *Geophys. Res. Lett.* **12**, 2405–2408.

Santer, B. D., Taylor, K. E., Wigley, T. M. L., Johns, T. C., Jones, P. D., Karoly, D. J., Mitchell, J. F. B., Oort, A. H., Penner, J. E., Ramaswamy, V., Scharzkopf, M. D., Stouffer, R. J., and Tett, S.: 1996, 'A Search for Human Influences on the Thermal Structure of the Atmosphere', *Nature* **382**, 39–46.

Sassen, K., Starr, D. O., Mace, G. G., Poellot, M. R., Melfi, S. H., Eberhard, W. L., Sphinhirne, J. D., Elorante, E. W., Hagen, D. E., and Hallet, J.: 1995, 'The 5–6 December 1991 FIRE II Jet Stream Cirrus Case Study: Possible Influences of Volcanic Aerosols', *J. Atmos. Sci.* **52**, 97–132.

Sato, M., Hansen, J. E., McCormick, M. P., and Pollack, J. B.: 1993, 'Stratospheric Aerosol Optical Depth, 1850–1990', *J. Geophys. Res.* **98**, 22,987–22,994.

Schönwiese, Ch. D.: 1994, 'Analysis and Prediction of Global Climate Temperature Change Based on Multiforced Observational Statistics', *Environ. Pollut.* **83**, 149–154.

Stott, P. A., Tett, S. F. B., Jones, G. S., Allen, M. R., Ingram, W. J., and Mitchell, J. F. B.: 2001, 'Attribution of Twentieth Century Temperature Change to Natural and Anthropogenic Cause', *Clim. Dyn.* **17**, 1–21.

Stott, P. A., Tett, S. F. B., Jones, G. S., Allen, M. R., Mitchell, J. F. B., and Jenkins, G. J.: 2000, 'External Control of 20th Century Temperature by Natural and Anthropogenic Forcings', *Science* **290**, 2133–2137.

Svensmark, H. and Friis-Christensen, E.: 1997, 'Variation of Cosmic Ray Flux and Global Cloud Coverage – a Missing Link in Solar-climate Relationships', *J. Atmos. Solar-Terr. Phys.* **59**, 1225–1232.

Thomson, D. J.: 1995, 'The Seasons, Global Temperature, and Precession', *Science* **268**, 59–68.

Wang, P. H., Minnis, P., and Yue, G. K.: 1995, 'Extinction Coefficient (1 μm) Properties of High-altitude Clouds from Solar Occultation Measurements (1985–1990): Evidence of Volcanic Aerosol Effect', *J. Geophys. Res.* **100**, 3181–3199.

(Received 20 July 2001; in revised form 22 March 2002)